JACS
JOURNAL OF THE AMERICAN CHEMICAL SOCIETY

Article

pubs.acs.org/JACS

Unravelling the Key Driving Forces of the Spin Transition in π-Dimers of Spiro-biphenalenyl-Based Radicals

Maria Fumanal, Fernando Mota, Juan J. Novoa, and Jordi Ribas-Arino*

Departament de Química Física and IQTCUB, Facultat de Química, Universitat de Barcelona, Avinguda Diagonal 645, 08028 Barcelona, Spain

Supporting Information

ABSTRACT: Spiro-biphenalenyl (SBP) boron radicals constitute an important family of molecules for the preparation of functional organic materials. The building blocks of several SBP-based crystals are π-dimers of these radicals, in which two phenalenyl (PLY) rings face each other and the other two PLYs point away from the superimposed PLYs. The dimers of ethyl-SBP and butyl-SBP undergo a spin transition between a diamagnetic and a paramagnetic state upon heating, while other dimers exhibit paramagnetism at all temperatures. Here, we present a computational study aimed at establishing the driving forces of the spin-transition undergone by ethyl-SBP at ∼140 K. The ground state of the π-dimers below 140 K is a singlet state in which the SBP unpaired electrons are partially localized in the superimposed PLYs. Above 140 K, the unpaired electrons are localized in the nonsuperimposed PLYs. These high-temperature structures are exclusively governed by the ground triplet state because the open-shell singlet with the unpaired electrons localized in the nonsuperimposed PLYs does not feature any minimum in the potential energy surface of the system. Furthermore, we show that the electrostatic component of the interaction energy between SBP radicals in the π-dimers is more attractive in the triplet than in the singlet, thereby partially counteracting the bonding and dispersion components, which favor the singlet. This electrostatic stabilization of the triplet state is a key driving force of the spin transition of ethyl-SBP and a key factor explaining the paramagnetic response of the π-dimers of other SBP-based crystals.

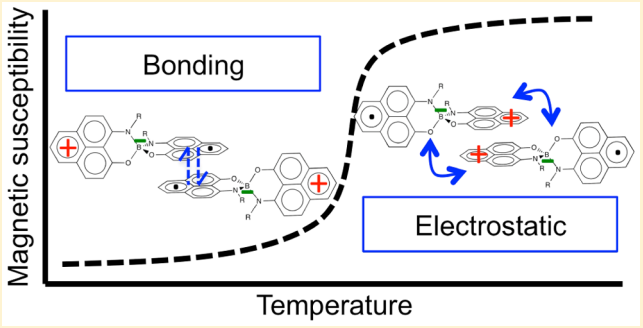

INTRODUCTION

Organic radicals have been and still are the subject of extensive investigations in view of their huge potential in the fabrication of future nanoscale electronic devices and the design of new functional materials.[1−4] Phenalenyl (PLY), which is an odd-alternant hydrocarbon arising from a triangular fusion of three benzene rings, is one of the most prominent neutral radicals. The potential of this neutral radical to serve as a building block for organic metals and superconductors was originally recognized by Haddon in 1975.[5] Since then, phenalenyl derivatives have furnished enthralling examples of spin-mediated molecular functionalities[6] (such as molecular switches,[7] molecular-scale memories[8] or spin quantum bits[9]), single-component molecular conductors,[10] thermochromic compounds,[11] and materials that change their magneto-optical-electronic properties upon phase transition.[12]

Within the family of phenalenyl radicals, the numerous spiro-biphenalenyl (SBP) boron radicals reported by Haddon and co-workers[10,12−27] constitute one of the most prominent sets of open shell molecules. SBPs present two nearly perpendicular phenalenyl units connected through a boron spiro-linkage. Such phenalenyl units are linked to the boron atom through oxygen or nitrogen atoms. Electrochemistry and ESR studies showed that these molecules feature a considerable charge separation that leads to a −1 tetracoordinated-boron atom and a symmetrically delocalized +1 positive charge accompanied by an unpaired electron.[13,28]

The N- and O-functionalized SBPs (i.e., SBPs in which each phenalenyl unit is bonded to the central boron atom via an oxygen and a nitrogen atom, see Figure 1a) exhibit diverse packing motifs in the solid state and, hence, different physical properties, depending on the substituents attached to the nitrogen atom (see Figure 1a). Ethyl and butyl-substituted SBPs present a crystal structure containing π-dimers as the basic building block (see Figure 1b) and show promise for memory or sensor applications because they undergo a phase transition upon heating/cooling that brings about remarkable changes in several physical channels, such as conductivity, magnetism, color and IR transmittance.[12,14,29] The phase transition of ethyl-SBP is reversible and is detected at about 140 K, while that of butyl-SBP occurs above room temperature and is accompanied by an hysteresis loop of about 25 K.

In both ethyl- and butyl-SBPs, the phase detected at low temperatures is diamagnetic, while the high-temperature phase is paramagnetic. The different magnetic response of the two

Received: April 20, 2015
Published: September 18, 2015

DOI: 10.1021/jacs.5b04053
J. Am. Chem. Soc. 2015, 137, 12843−12855

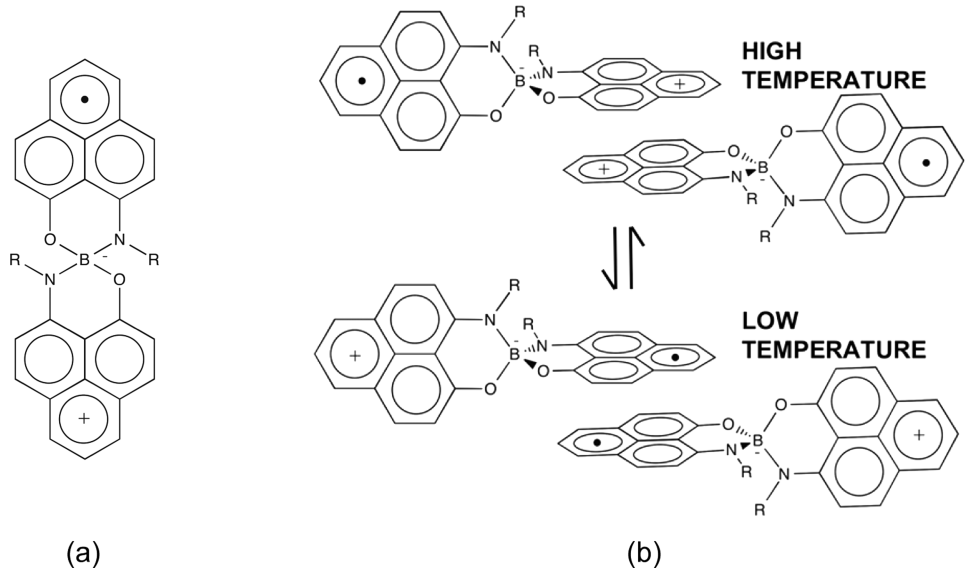

Figure 1. (a) Scheme of a N- and O-functionalized spiro-bis(1,9-disubstitutedphenalenyl) boron radical. (b) Scheme of the high-temperature (above) and low-temperature (bottom) electronic states of a π-dimer of spiro-bisphenalenyl neutral radicals.

phases was ascribed to an intramolecular electron transfer upon phase transition.[12] A bond-length analysis conducted on the X-ray crystal structures of ethyl- and butyl-SBP at different temperatures[30,31] showed that in the low-spin (LS) state of the π-dimers of SBP, the unpaired electrons of each phenalenyl are partially localized on the phenalenyl units directly involved in the π-dimer (i.e., the superimposed phenalenyl moiety, see Figure 1b) and couple to form a magnetically silent state. Conversely, the same bond-length analysis revealed that in the high-spin (HS) state of the π-dimers, the SBP unpaired electrons are localized mainly on the phenalenyl unit not directly involved in the π-dimer (i.e., the nonsuperimposed phenalenyl moiety, see Figure 1b).[30,31]

The LS states of the π-dimers of ethyl and butyl-SBP present structural and magnetic properties in close analogy to those observed for the π-dimer of the neutral radical 2,5,8-tri*t*-butyl-phenalenyl (TBPLY).[32] These dimers present seven eclipsed interfragment C···C contacts, with distances significantly shorter than twice the van der Waals radius of carbon atom. The energy gap between the ground singlet state and the first triplet state in these dimers is ca. 4 kcal/mol,[33,34] which indicates a very strong antiferromagnetic coupling between the two unpaired electrons within each π-dimers. The strong bonding between phenalenyl units in the TBPLY π-dimers is also reflected in the experimental enthalpy change upon dimerization in dichloromethane, which is ca. −10 kcal/mol.[35] Theoretical analysis[35,36] and spectroscopic studies[37] indicated that the intriguing structural and physical properties of the TBPLY dimers originate in a long, multicenter bond (alternatively called *pancake* bond[38]) between the two phenalenyl units of the dimer. Although the dominant attractive component of the interaction energy in TBPLY dimers is the dispersion component,[36] the covalent-like properties of these dimers arise from a strong overlap between the SOMO orbital of each phenalenyl unit. The SOMO−SOMO bonding component of such interaction energy has been estimated to be ca. −13 kcal/mol.[36]

Analogously to the packing motif found in TBPLY dimers, the π-dimers between the superimposed phenalenyl units of the LS states of ethyl and butyl-SBP also feature seven quasi-eclipsed interfragment C···C contacts with intermolecular distances shorter than the sum of the van der Waals radii. Concerning the magnetic properties, the coupling between unpaired electrons of the superimposed phenalenyl units in the LS states of ethyl and butyl-SBP is strongly antiferromagnetic,[39] as in TBPLY dimers. Given the close similarities between the TBPLY and SBP dimers, it can be inferred that the bond between the superimposed phenalenyl units of ethyl and butyl-SBP in their LS states should be described as a long, multicenter bond. Hence, the origin of the stability of these dimers in their LS states is expected to arise mainly from dispersion and also from a SOMO−SOMO overlap energetic component.

The thermal spin transitions undergone by ethyl and butyl-SBP indicate that the HS states of the π-dimers of these systems must be fairly close in energy to the LS states (especially in the case of ethyl-SBP, for which the spin transition occurs at about 140 K). Otherwise, the higher entropy of the HS states would not suffice to clear the adiabatic energy gap (ΔE_{adiab}) between the HS and LS states. Nevertheless, the reasons for which these HS states should lie so close in energy to the LS states are not yet well understood for the following three considerations. First and foremost, the charge distribution present in the HS states, where two delocalized positive charges face each other (see Figure 1b), should in principle lead to a considerable electrostatic destabilization of the HS states and thus to an increase of ΔE_{adiab}. Second, the attractive SOMO−SOMO bonding component present in the LS states is zero in the HS states because the two unpaired electrons of the π-dimers are in their higher spin multiplicity state (in this case, a triplet state). In view of the large bonding component estimated for the TBPLY dimer (see above), one would expect a large stabilization of the LS states (relative to the HS states) and thus a large value of ΔE_{adiab}. Last, the interplanar distance between superimposed phenalenyl units increases by about 0.1 Å in going from LT to HT, and this might easily entail a weakening of the dispersion component of the interaction energy of SBPs in the π-dimers, thereby increasing the value of ΔE_{adiab}. These three considerations (especially the first one) thus prove that it is not yet fully understood why the π-dimers

DOI: 10.1021/jacs.5b04053
J. Am. Chem. Soc. 2015, 137, 12843−12855

of ethyl- and butyl-SBP can undergo a thermally driven spin transition that drives these dimers to a HS state that one would intuitively expect to be thermally inaccessible. In fact, these considerations also lead to two other key questions: (i) what prevents the π-dimers from dissociating in the HS state?, and (ii) why do the SBP unpaired electrons prefer to localize in the nonsuperimposed PLY rings in the HS state? Let us stress that addressing these issues is not only highly relevant in the case of ethyl- and butyl-SBP but also for other members of the family of SBP-based compounds. Indeed, there are four other SBP-based crystals containing π-dimers in which the SBP unpaired electrons are localized in the nonsuperimposed PLY rings in the whole range of temperatures.[15,16,18,27] In these cases, it is observed that the HS state is thermally populated at all temperatures.

The unresolved issues concerning the HS states reflect that the spin transitions undergone by ethyl- and butyl-SBP and, in broader terms, the electronic structure of the π-dimers of other SBP-based radicals, are not completely understood yet. Given that the physical properties (conductivity, magnetic and optical properties) of SBP-based materials comprising π-dimers depend on the electronic structure of these building blocks, it is clear that achieving a detailed understanding of the factors controlling this electronic structure is of paramount importance. Despite the computational works carried out to rationalize the change in magnetism and conductivity of the different phases of the switchable SBP-based materials[39−42] and the theoretical studies on other phenalenyl-based systems,[34−37,43−48] the electronic structure of the LS and HS states at the molecular level has never been investigated in detail using wave function methods. The potential energy surfaces of the LS and HS electronic states have never been explored either. In this computational work, we address all these issues by studying the π-dimers of ethyl-SBP and we reveal the key driving forces underlying the spin-transition undergone by this material. Anticipating our results, we uncover that the intermolecular electrostatic interactions between SBP radicals within the π-dimers plays a prime role in defining the electronic structure of the HS states and in driving the spin-transition. The results obtained for ethyl-SBP offer also valuable insight into the spin-transition of butyl-SBP and allow for a rationalization of the electronic structure of the π-dimers of other SBP-based materials, specifically, those dimers in which the SBP unpaired electrons are localized in the non-superimposed PLY rings over the whole range of temperatures.

RESULTS AND DISCUSSION

The presentation of the results is organized as follows. We will first inspect the electronic structure of an isolated spirobiphenalenyl neutral radical (Subsection 1). Then, we will examine the electronic structure of the π-dimers extracted from the X-ray crystal structures of ethyl-SBP at different temperatures (Subsection 2). After that, we will explore the topology of the potential energy surface of the SBP π-dimers (Subsection 3). Finally, we will demonstrate that the intermolecular electrostatic interactions between SBP radicals within the π-dimers play a central role in shaping the electronic structure of these dimers and driving their spin-transition (Subsection 4).

(1). Electronic Structure of a Spirobiphenalenyl Neutral Radical. In order to properly understand the electronic structure of the π-dimers of ethyl-SBP, the nature of the electronic ground state of its constituent monomers must be examined first. SBP radicals are purely organic mixed-valence compounds[49,50] because they comprise two redox centers (the two PLY units) that can be found, formally, in two different oxidation states (either as a cationic unit or as a neutral unit with one unpaired electron, see Figure 1a). As with other mixed-valence compounds, the key question regarding the electronic structure of these radicals is whether in their electronic ground state the unpaired electron (or, alternatively, the positive charge) is localized in a single phenalenyl unit or whether it is delocalized over the two phenalenlyl units.

Organic redox centers usually have different geometries depending on their oxidation state. In the particular case of a phenalenyl unit, the bond lengths of its cation are significantly different from those of its neutral radical.[17] This can be understood on the basis of the spatial topology of the singly occupied molecular orbital (SOMO) of a single phenalenyl unit[28] (Figure 2a). The bond lenghts in the neutral radical are

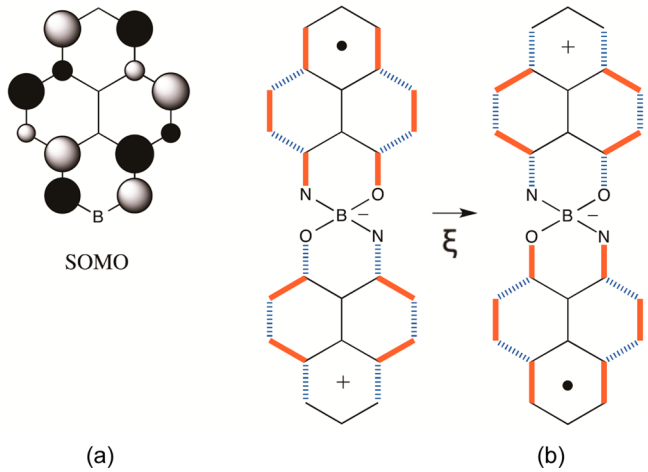

Figure 2. (a) Topology of the SOMO of one of the phenalenyl units in a SBP radical. (b) Scheme of the two asymmetric spin localized structures of a SBP neutral radical. In the scheme on the left (right), the unpaired electron is localized in the upper (lower) phenalenyl, while the positive charge is localized in the lower (upper) phenalenyl. ξ denotes the reaction coordinate of the electron transfer from the upper phenalenyl to the lower one. The distances of the bonds highlighted in orange on the structure on the left and highlighted with blue lines on the structure on the right decrease upon electron transfer. Conversely, the distances of the bonds highlighted with blue lines on the structure on the left and highlighted in orange on the structure on the right increase upon electron transfer. The distances of those bonds marked with a black line do not change significantly upon electron transfer.

shorter or longer (as compared with the cation) depending on the bonding or antibonding character of the SOMO. For instance, the antibonding character of this SOMO along the C−N and C−O bonds explains why these bonds are shorter in the cation than in the neutral radical.[17] These observations, in turn, strongly suggest that the bond lengths in a SBP radical are determined by the degree of (de)localization of its SOMO. If this were the case, an electronic ground state with a completely delocalized unpaired electron would result in the two phenalenyl units having the same bond lengths. On the contrary, an electronic ground state with the unpaired electron completely localized on one of the phenalenyls would result in one phenalenyl having the bond distances of the neutral radical and the other phenalenyl having the bond distances of the cationic species.

DOI: 10.1021/jacs.5b04053
J. Am. Chem. Soc. 2015, 137, 12843−12855

The presumed interplay between the (de)localization of the unpaired electron within a SBP radical and the geometry of its redox centers can be used to compute the potential energy profile along the reaction coordinate associated with an electron transfer from one phenalenyl unit to the other. The evaluation of such an energy profile will allow us to ascertain the degree of (de)localization of the unpaired electron in the electronic ground state of an SBP molecule. In order to compute such profile, we first obtained the optimized structures associated with the electronic configurations having the unpaired electron localized in either one or the other phenalenyl unit. Then, we obtained an approximation of the exact reaction path of the electron transfer process by generating a set of molecular geometries through a linear interpolation between the two previously optimized asymmetric spin localized structures (Figure 2b). This set of molecular geometries along the reaction coordinate of the electron transfer (ξ) includes a symmetric structure in which the geometries of both phenalenyl units are the same.

Single point CASSCF(1,2) calculations performed on every geometry along ξ show that the spin density distribution over the two phenalenyls changes along this reaction coordinate. As displayed in Figures 3 and 4 (see also Table S1), the symmetric geometry featuring two structurally identical phenalenyl units leads to an unpaired electron delocalized over the two redox centers. Conversely, those asymmetric geometries in which the bond distances of one of the PLY units correspond to a PLY

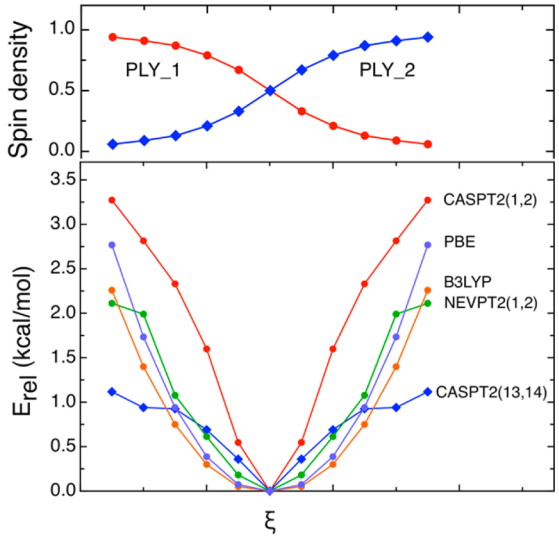

Figure 3. (Top) Evolution of the spin density distribution over the two PLY units of an isolated SBP radical along the reaction coordinate associated with the electron transfer between the two PLYs (ξ), as computed by means of CASSCF(1,2) calculations. PLY_1 (PLY_2) denotes the upper (lower) phenalenyl unit depicted in Figure 2b. (Bottom) Adiabatic energy profiles along ξ, as computed with different electronic structure methods. The leftmost (rightmost) points of both graphics correspond to the leftmost (rightmost) SBP structure depicted in Figure 2b (i.e., to the asymmetric structures). The midpoints of the profiles correspond to the symmetric structures with two structurally identical PLY units. Note that the curve displaying the CASPT2(13,14) results in the bottom graphic is meant to prove that larger active spaces confirm the delocalized ground state obtained in the CASPT2 calculations with the minimal active space (i.e., the CASPT2(1,2) calculations). The data in both graphics are connected with lines to guide the eye.

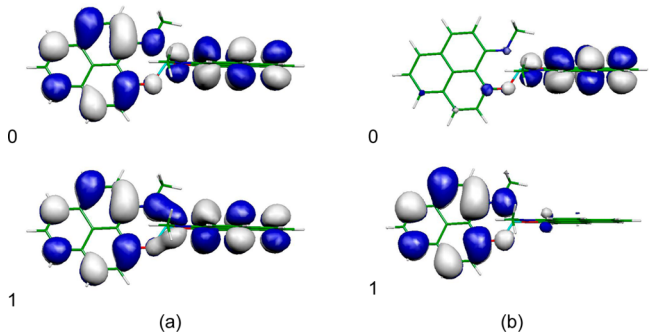

Figure 4. Natural orbitals and the corresponding occupation numbers (indicated on the left) obtained from CASSCF(1,2) calculations on a SBP radical for (a) a symmetric structure and (b) an asymmetric spin localized structure.

radical and the bond distances of the other PLY unit correspond to a PLY cation lead to a localization of the spin density on the PLY unit having the bond distances of the PLY radical. Our analysis thus proves that the degree of spin (de)localization in a SBP radical and the bond distances of its two phenalenyl units are intertwined, thereby providing a theoretical support to the previously reported use of the bond lengths of the PLY units to describe the electronic structure of the π-dimers of ethyl- and butyl-SBP based on crystallographic data.[17,30,31]

The energy profile obtained upon performing single-point CASPT2 and NEVPT2 calculations on the different geometries along ξ is a single well profile with the energy minimum found at the geometry that features two structurally identical PLY units (see Figure 3 and also Figure S1). It thus follows that in the electronic ground state of an SBP radical the unpaired electron is completely delocalized over its two PLY moieties. In other words, our ab initio study demonstrates that an isolated N- and O-functionalized SBP boron radical belongs to the Robin-Day[51] Class III of mixed-valence compounds. The delocalized electronic ground state found in our gas-phase calculations is consistent with the results obtained in cyclic voltammetry experiments, and solution phase ESR measurements.[13]

Concerning the performance of density functional theory when it comes to describing the electronic structure of an isolated SBP radical, Figure 3 shows that both the PBE[52] and B3LYP[53] exchange-correlation functionals provide a single well potential for the energy profile of the electron transfer process between PLY units of a SBP radical (see also Table S1). On the other hand, full geometry optimizations of the SBP radical with these two functionals furnished a structure with the unpaired electron symmetrically delocalized over the two PLY units. The good agreement of the results obtained at the B3LYP and PBE levels with those obtained with correlated wave function methods proves that these functionals can provide a proper description of the electronic structure and the topology of the potential energy surface of the π-dimers of SBPs (see next subsections).

To conclude this subsection, let us stress that the analysis herein presented not only paves the way for the study of the electronic structure of the π-dimers of ethyl-SBP but also brings to light a feature that is crucial to understand the large variety of electronic structures (in terms of the degree of (de)localization of the unpaired electron) observed in the SBP radicals of SBP-based organic conductors. Indeed, our calculations reveal that

DOI: 10.1021/jacs.5b04053
J. Am. Chem. Soc. 2015, 137, 12843−12855

despite the symmetric delocalization of the unpaired electron in the ground state of SBP, a complete localization of the spin density on one of the redox centers entails a very small energy cost of about 1−2 kcal/mol. Such a small energy penalty explains why the degree of (de)localization of the unpaired electron in a SBP radical can be so easily altered in the solid state by virtue of intermolecular interactions, thereby providing an appealing rationale for the large diversity of electronic structures observed within the family of SBPs, including three SBP derivatives that feature an asymmetric electron density distribution in spite of being monomeric in the solid state.[13,20,30]

(2). Electronic Structure of the X-ray Crystal Structures of π-Dimers of SBP. After the analysis of the electronic structure of an isolated SBP radical, we will focus on the electronic structure that arises from the dimerization of these radicals. In this subsection, we shall analyze the degree of (de)localization of the unpaired electrons over the PLY units of the radicals of the π-dimers extracted from the X-ray crystal structures of ethyl-SBP at different temperatures (including temperatures below and above the phase transition temperature).[30] Note that all results presented in this subsection were obtained using the dimer structures directly excised from the X-ray crystal structures without any geometry optimization. The C_i symmetry of the X-ray crystal structures of the π-dimers was preserved and exploited in all the calculations.

The computed energy spectrum of the π-dimers of ethyl-SBP (Figure 5) reveals that the electronic ground state at all

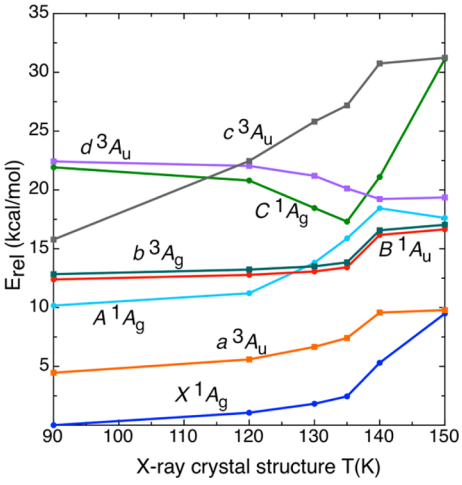

Figure 5. Energy spectra of the four lowest-lying singlet states and the four lowest-lying triplet states of a π-dimer of ethyl-SBP as a function of temperature, as obtained with single-point NEVPT2(2,4)/6-31G(d) calculations using X-ray crystal structures recorded at different temperatures. All the energies are given relative to the energy of the lowest-lying ^1A_g state at the crystal geometry refined at 90 K. The data are connected with lines to guide the eye.

temperatures is a singlet state of A_g symmetry (^1A_g). The electronic state that lies closer to the ground state (specially at higher temperatures, see Figure 5) is a triplet state of A_u symmetry (^3A_u). The rest of excited states lie quite high in energy with respect to the ^1A_g ground state and are thus not expected to play any role in driving the spin transition of ethyl-SBP. Hence, only the lowest lying ^1A_g and ^3A_u states will be considered hereafter.

For all the X-ray structures of the π-dimers, the natural orbitals obtained from CASSCF(2,4) calculations were found to be essentially localized either on the superimposed PLY units or on the nonsuperimposed PLY units (Figure 6). The subset

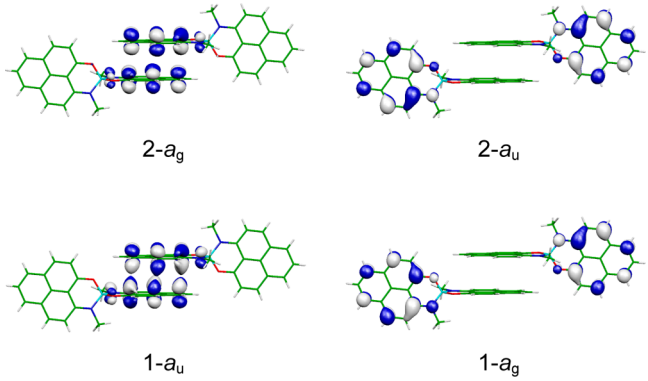

Figure 6. Natural orbitals obtained from CASSCF(2,4) calculations of the π-dimer of ethyl-SBP. The displayed orbitals are those included in the active space of these calculations.

of orbitals centered on the superimposed PLY units includes one orbital of bonding character of a_u symmetry and another orbital of antibonding character of a_g symmetry. The subset of orbitals localized on the nonsuperimposed PLY units, in turn, includes two orbitals of nonbonding character, one of them of a_g symmetry and the other one of a_u symmetry (Figure 6).

The localized character of the natural orbitals renders the characterization of the wave function straightforward once the occupations of these natural orbitals are known. The occupation numbers for the X-ray structures at different temperatures (Table 1; see also Table S2 for the occupation numbers of the excited states) prove that below 135 K (i.e., below the spin transition temperature), the unpaired electrons of SBPs in the ^1A_g ground state are mainly localized on the superimposed PLY units of the π-dimers, but there is a partial delocalization over the nonbonding orbitals of the nonsuperimposed PLYs, which increases as the crystal temperature does. These observations are in line with the electron distributions obtained on the basis of an experimentally based structural analysis.[30] As for the ^3A_u state, our analysis shows that in the 90−110 K temperature range, this triplet state has one unpaired electron in the superimposed PLYs and the other unpaired electron in the nonsuperimposed PLYs (Table 1). Note, however, that in this temperature range the triplet lies ca. 5 kcal/mol higher than the ground singlet state (Figure 5), and, consequently, it is not thermally populated.

Above 140 K (i.e., above the spin transition temperature), the unpaired electrons in both the ^1A_g and ^3A_u states are completely localized on the nonbonding orbitals of the nonsuperimposed PLY units (Table 1). The observed localization of spin density on the nonsuperimposed PLY units is mantained at all temperatures up to room temperature and is also in good agreement with the experimental data,[30] which shows such localization for temperatures above about 200 K.

In summary, the electronic structure of SBPs changes substantially upon dimerization. If this dimerization did not give rise to any polarization of the charge density, the unpaired electrons would be completely delocalized over the four PLY units (see top scheme of Figure 7). In contrast, our calculations show that the dimerization results in a partial localization of the

DOI: 10.1021/jacs.5b04053
J. Am. Chem. Soc. 2015, 137, 12843−12855

Table 1. Evolution of the Electronic Structure of the X-ray Crystal Structures of the π-Dimers of Ethyl-SBP as a Function of Temperature[a]

^1A_g state	90K	100K	110K	120K	130K	135K				
NO[b] 1-a_g	0.16	0.16	0.17	0.17	0.19	0.22	0.39	0.83	0.85	0.86
NO 2-a_g	0.00	0.00	0.00	0.00	0.00	0.00	0.00	0.00	0.00	0.00
NO 1-a_u	1.66	1.65	1.64	1.63	1.60	1.57	0.14	0.01	0.01	0.01
NO 2-a_u	0.19	0.19	0.20	0.20	0.21	0.21	1.47	1.16	1.15	1.14
^3A_u state							140K	150K	160K	170K
NO 1-a_g	0.98	0.98	0.98	0.98	0.99	0.99	1.00	1.00	1.00	1.00
NO 2-a_g	0.02	0.02	0.02	0.02	0.01	0.01	0.00	0.00	0.00	0.00
NO 1-a_u	0.98	0.98	0.98	0.50	0.01	0.01	0.00	0.00	0.00	0.00
NO 2-a_u	0.02	0.02	0.02	0.50	0.99	0.99	1.00	1.00	1.00	1.00
Calculated Phenalenyls Electronic population[c]										
S	0.83	0.82	0.82	0.81	0.80	0.79	0.00	0.00	0.00	0.00
NS	0.17	0.18	0.18	0.19	0.20	0.21	1.00	1.00	1.00	1.00
Experimental Phenalenyls Electronic population[d]										
S	0.65	0.63	0.61	0.57	0.49	0.42	0.17	0.14	0.11	0.06
NS	0.35	0.37	0.39	0.43	0.51	0.58	0.83	0.86	0.89	0.94

[a]The electronic structure for the lowest ^1A_g and ^3A_u states is described in terms of the occupations of the natural orbitals displayed in Figure 6. The calculated electronic population on the superimposed (S) and nonsuperimposed (NS) PLY units is compared with the results obtained from the experimentally based structural analysis of Ref 30. [b]NO stands for Natural Orbital. [c]These electronic populations were computed on the basis of the occupation of the natural orbitals displayed in Figure 6. Since these natural orbitals are localized either on the superimposed (S) or the nonsuperimposed (NS) PLY rings, the partition of the electron population into a contribution on the S PLY units and another contribution on the NS PLY units is straightforward. Note that these populations are given for only one SBP radical of the corresponding π-dimer (due to the C_i symmetry of the π-dimer, the electron distribution of both SBP radicals in the π-dimer is exactly the same). [d]Data taken from ref 30.

unpaired electrons on the superimposed PLY units below the spin transition temperature, and in a localization of the unpaired electrons on the nonsuperimposed PLY units above the spin transition temperature (Figure 7). It should be mentioned that the changes in the electronic structure of the π-dimers of butyl-SBP upon spin transition are completely analogous to those described for the π-dimers of ethyl-SBP (see Table S3).

To conclude this subsection, it is interesting to compare the electronic structure of the ^1A_g ground state of the π-dimer of SBP with that of the singlet ground state of the π-dimer of TBPLY.[36] In both cases, the ground singlet state has a marked multiconfigurational character and the orbital with the largest occupation is the orbital featuring the bonding combination of the SOMOs (in the case of ethyl-SBP, the SOMOs of the superimposed PLYs). However, there is a crucial difference between the two cases. In the π-dimer of TBPLY (like in the π-dimers of other radicals, such as TCNE[36]), the orbital associated with the antibonding combination of the SOMOs has a significant occupation. By contrast, the occupation of the orbital of antibonding character centered on the superimposed PLY rings (i.e., the 2-A_g orbital in Figure 6) in the ^1A_g state is zero over the whole range of temperatures. The partial occupation of the nonbonding orbitals centered on the nonsuperimposed PLYs reflects the tendency of the SBP radicals to delocalize their unpaired electrons over their two PLY units. The analysis herein presented thus demonstrates that the electronic structure of the SBP π-dimer in their singlet ground state is the result of the subtle competition between the delocalized ground state of isolated SBP radicals and the SOMO−SOMO overlap, which favors the localization of the unpaired electrons in the superimposed PLYs. The key question with which we are left now in order to achieve a full understanding of the electronic structure of the π-dimer in ethyl-SBP is: which is the driving force responsible for the localization of the SBP unpaired electrons on the non-superimposed PLYs above the spin-transition temperature? We shall provide an answer to this question in the last subsection of this discussion.

(3). Exploration of the Potential Energy Surface of the π-Dimers of SBPs: Mechanism of the Spin-Transition. After the analysis of the electronic structure of the ^1A_g and ^3A_u electronic states, we shall now explore the topology of the corresponding potential energy surfaces (PES). We first carried out geometry optimizations of an isolated π-dimer at the B3LYP-D2 level. As shown in Table 2, the interplanar distance between superimposed PLYs is smaller in the minimum of the ^1A_g state (3.17 Å) than in the minimum of the ^3A_u state (3.21 Å). This significant increment of the interplanar separation in going from ^1A_g to ^3A_u is compatible with the abrupt change observed for this structural variable in the X-ray crystal structures of ethyl-SBP upon spin transition.[30] The bond distances in the PLY units of the optimized singlet state also differ from the bond distances obtained for the optimized triplet state. In fact, single point CASSCF(2,4) calculations on the B3LYP-D2 structural minima reveal that the pattern of bond distances in the optimum structure of ^1A_g brings about a

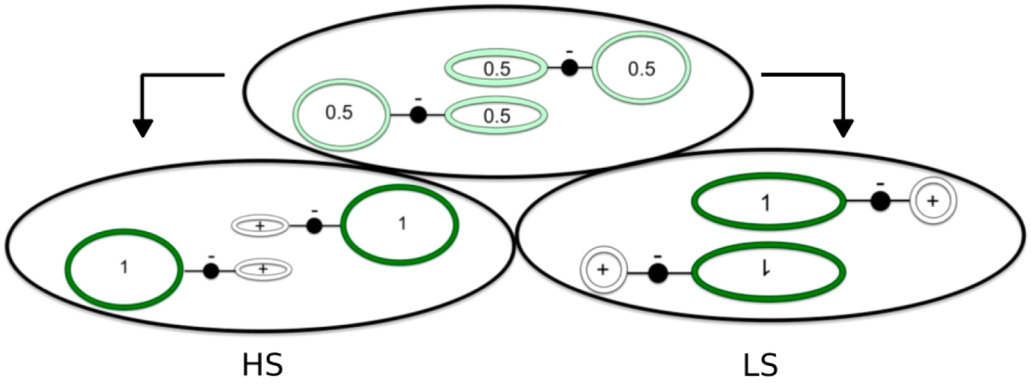

Figure 7. Scheme of the electronic structure of π-dimers of SBPs. If the formation of the dimer was not accompanied by any polarization of the charge densities, the unpaired electrons would be equally distributed over all the PLY units (top). In the low-spin (LS) state, there is a partial localization of the unpaired electrons on the superimposed PLY units. In contrast, in the high-spin (HS) state, the unpaired electrons of SBPs localize on the nonsuperimposed PLY units.

DOI: 10.1021/jacs.5b04053
J. Am. Chem. Soc. 2015, 137, 12843−12855

Table 2. Selected Structural Parameters for the SBP π-Dimers Present in Two Different X-ray Crystal Structures of Ethyl-SBP[a] and the Corresponding Structural Parameters Obtained upon Geometry Optimization of These SBP π-Dimers in Their ^1A_g and ^3A_u States Using Different Electronic Structure Methods[b]

	X-ray	B3LYP-D2[e]	PBE-D2[f]	PBE-D2[g]
	90 K	^1A_g	^1A_g	^1A_g
D[c]	3.241	3.168	3.187	3.162
C−N (S)[d]	1.354	1.355	1.362	1.361
C−O (S)	1.341	1.335	1.344	1.345
C−N (NS)	1.347	1.348	1.352	1.357
C−O (NS)	1.326	1.330	1.336	1.332
	140 K	^3A_u	^3A_u	^3A_u
D	3.341	3.214	3.273	3.232
C−N (S)	1.336	1.349	1.356	1.354
C−O (S)	1.329	1.329	1.338	1.340
C−N (NS)	1.362	1.354	1.358	1.363
C−O (NS)	1.339	1.336	1.341	1.338

[a]The values in the upper (lower) part of the Table correspond to the X-ray structure refined at 90 K (140 K). [b]All distances are given in angstroms. [c]D refers to the interplanar distance between the superimposed PLYs. D has been measured as the distance between the central carbon (i.e., the carbon atom shared by the three fused benzene rings) of the two superimposed PLY units. [d]C−N (S) and C−N (NS) denote the C−N bond distance of the superimposed and nonsuperimposed PLYs, respectively. C−O (S) and C−O (NS) denote the C−O bond distance of the superimposed and nonsuperimposed PLYs, respectively. [e]Calculations performed for isolated π-dimers using the 6-31G(d) basis set. [f]Calculations performed for isolated π-dimers using the 6-31G(d) basis set. [g]These PBE-D2 calculations were performed in the solid state (see Computational Details for further information).

localization of the SBP unpaired electrons on the superimposed PLYs, whereas the optimum structure of ^3A_u results in a localization of the unpaired electrons on the nonsuperimposed PLYs (see Table 3). It should also be mentioned that the optimized structural variables are in good agreement with the X-ray data (Table 2).

An attempt to obtain a minimum structure for the ^3A_u state with the SBP unpaired electrons localized on the superimposed PLYs led to the very same optimized structure for ^3A_u described in Table 2. This means that the configuration with the unpaired electrons localized on the superimposed PLYs does not exist as a minimum in the PES of the triplet ground state of an isolated π-dimer of SBP. Likewise, an attempt to obtain a minimum structure for the ^1A_g state with the SBP unpaired electrons localized on the nonsuperimposed PLYs led to the very same optimized structure for ^1A_g described in Table 2. In other words, upon optimization of the open shell singlet with the unpaired electrons localized in the nonsuperimposed PLYs, it is observed that the unpaired electrons flow from the nonsuperimposed PLYs to the superimposed PLYs in a barrierless process (NEVPT2 calculations validate this result; see Figure S2). It thus follows that the configuration with the unpaired electrons localized on the nonsuperimposed PLYs does not exist as a minimum in the PES of singlet ground state of an isolated π-dimer of SBP. Let us stress that structure optimizations of ethyl-SBP in the solid-state perfomed at the PBE-D2 level confirm this result (Table 2; see also Figure S3).

Table 3. Electronic Structure in Terms of the Occupations of the Natural Orbitals Displayed in Figure 6 for the SBP π-Dimers Present in Two Different X-ray Crystal Structures of Ethyl-SBP and for the Geometries Obtained upon Geometry Optimization of These SBP π-Dimers in their ^1A_g and ^3A_u States Using Different Electronic Structure Methods

	X-ray	B3LYP-D2	PBE-D2
^1A_g State	90 K	^1A_g Minimum	^1A_g Minimum
NO 1-a_g	0.16	0.14	0.12
NO 2-a_g	0.00	0.00	0.00
NO 1-a_u	1.66	1.67	1.69
NO 2-a_u	0.19	0.20	0.19
^3A_u State	140 K	^3A_u Minimum	^3A_u Minimum
NO 1-a_g	1.00	0.99	0.99
NO 2-a_g	0.00	0.01	0.01
NO 1-a_u	0.00	0.01	0.01
NO 2-a_u	1.00	0.99	0.99

The computed adiabatic energy gap between the minima of the ^3A_u and the ^1A_g states of an isolated π-dimer of SBP at the B3LYP-D2 level was found to be 1.6 kcal/mol (the singlet state being the most stable one). It is worth mentioning that the adiabatic gaps for an isolated π-dimer and for a π-dimer in the solid state are very similar (2.7 and 2.6 kcal/mol, respectively, according to PBE-D2 calculations). Taking also into account that the bond lengths within the PLYs of an isolated π-dimer are very similar to those of a π-dimer in the crystal lattice (Table 2), it is clear that the intermolecular interactions in the crystal lattice of ethyl-SBP do not significantly affect the electronic structure of its π-dimers.

At the optimum geometry of the ^3A_u state (in which the nonsuperimposed PLYs host the unpaired electrons), the singlet state lies 1.3 kcal/mol lower in energy (according to B3LYP-D2) than the triplet state, even if the singlet state does not feature any stationary point in that region of the PES. At the crystal structure of 150 K (i.e., above the spin transition temperature), in turn, B3LYP-D2 predicts that the triplet lies 0.5 kcal/mol higher in energy than the singlet, which is in agreement with the results by Kertesz and co-workers of ref 39.

The inspection of the PES herein presented provides valuable insight into the mechanism of the spin-transition in ethyl-SBP. On the basis of the experimental observations so-far reported for this system, two different scenarios were conceivable in terms of the topology of the PES of the lowest-lying singlet state. The first possible scenario draws on the hypothesis that the ^1A_g state features two different minima in the PES of the system (leftmost scheme in Figure 8). In this particular case, one minimum would be characterized by a localization of the unpaired electrons of the SBPs in the superimposed PLYs, while the other minimum would be characterized by a localization of the unpaired electrons in the nonsuperimposed PLYs. In this scenario, the π-dimers would hop from the former minimum to the latter one by virtue of an intramolecular electron transfer upon phase transition. The magnetic signal detected after the phase transition would originate in the population of the ^3A_u state, which lies very close in energy to the singlet ground state (leftmost scheme in Figure 8). The second possible scenario draws on the hypothesis that the ^1A_g state features only one minimum in the PES of the system and that the unpaired electrons are hosted in the superimposed PLYs in this minimum (rightmost scheme in Figure 8). In this scenario, the π-dimers would hop from the ^1A_g minimum to the ^3A_u minimum by virtue of an intramolecular electron transfer upon phase transition. In this

DOI: 10.1021/jacs.5b04053
J. Am. Chem. Soc. 2015, 137, 12843−12855

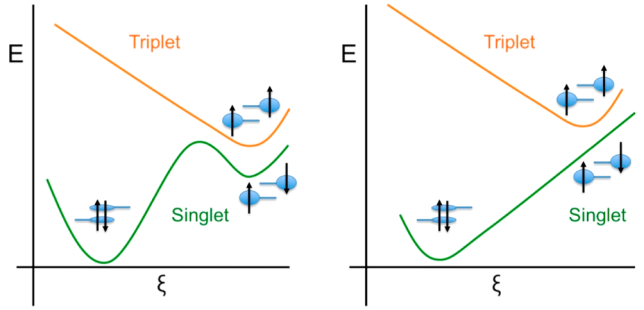

Figure 8. Scheme of two possible mechanistic scenarios for the spin transition of π-dimers of SBP in terms of two different topologies of the PES of the ^1A_g state. Schemes of the adiabatic potential energy curves for the ^1A_g and ^3A_u states along the reaction coordinate that drives the spin transition. In both schemes, the ^3A_u state features a single minimum, in which the nonsuperimposed PLYs host the unpaired electrons. In the scheme on the left, it is assumed that the ^1A_g state has two different minima (one with the unpaired electrons localized in the superimposed PLYs and the other one with the unpaired electrons localized in the nonsuperimposed PLYs). In the scheme on the right, it is assumed that the ^1A_g state has only one minimum, in which the unpaired electrons are localized in the superimposed PLYs. Our calculations have revealed that the correct mechanistic scenario is that depicted on the right.

case, the geometry of the π-dimers above the spin-transition temperature would be determined by the PES of the ^3A_u state because the PES of the ^1A_g state does not present any minimum associated with an electron distribution in which the unpaired electrons are localized in the nonsuperimposed PLYs (rightmost scheme in Figure 8).

Our work reveals that the correct scenario is the second one. However, the rightmost scheme in Figure 8 does not provide a complete picture of the spin-transition of ethyl-SBP. Indeed, this scheme does not take into account the vibrational entropy. As displayed in Figure 9, the $^1A_g \rightarrow {}^3A_u$ spin transition entails a

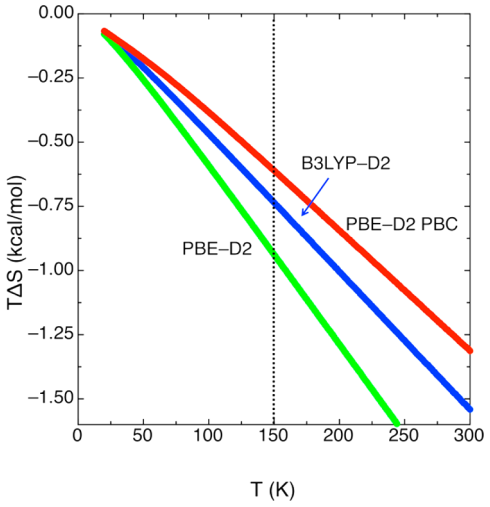

Figure 9. Temperature dependence of the difference in entropy (expressed as $T\Delta S$) between the lowest lying triplet and the lowest lying singlet states of π-dimers of SBP, as computed by means of different electronic structure methods. The blue and green curves correspond to calculations carried out for isolated SBP π-dimers. The red curve corresponds to calculations in the solid state, in which periodic boundary conditions (PBC) were imposed in all three directions.

vibrational entropy gain (i.e., the $T\Delta S$ term) of ca. 0.7 kcal/mol[54] at 150 K, which means that the vibrational entropy plays a crucial role in driving the spin-transition in ethyl-SBP.

Overall, the analysis herein presented reveals that the geometries of the π-dimers of ethyl-SBP above the spin-transition temperature are controlled by the PES of a triplet state whose single minimum energy configuration has the SBP unpaired electrons localized on the nonsuperimposed PLYs. The switching from the ^1A_g state to the ^3A_u state of the π-dimers is responsible for the sudden change of the interplanar distance between the superimposed PLYs and the sudden change in the bond lengths within the PLY rings observed upon phase transition. Remarkably, the open-shell singlet with the same electron distribution of the triplet state does not feature any minimum in the PES of the system. Yet this open-shell singlet state lies slightly lower in energy than the triplet state, thus explaining why the magnetic susceptibility measurements of ethyl-SBP indicate the presence of antiferromagnetic interactions above the spin transition.[39] Finally, let us emphasize that our calculations show that the π-dimers of ethyl-SBP in the triplet state are stable (against dissociation) not only in the condensed phase but also in the gas phase, even if there is no bonding between their unpaired electrons.

(4). Key Role of Electrostatic Interactions in Driving the Spin Transition. The small energy gap between the minima of the ^3A_u and the ^1A_g states reported in the previous subsection explains why ethyl-SBP can undergo a spin transition. Yet, the origin of such a small energy gap still remains elusive. In this subsection, we shall rationalize this central issue.

An interaction energy decomposition analysis performed on the B3LYP-D2 optimized structures of the ^1A_g and ^3A_u states of a π-dimer shows that the bonding and dispersion components of the interaction energy between SBPs result in a relative stabilization of the singlet state by about 2 and 1.4 kcal/mol, respectively (see Table S4). The bonding component favors the singlet state because it is associated with the pairing of the unpaired electrons of the SBP radicals. The smaller interplanar distance between superimposed PLYs in the ^1A_g minimum (compared to the ^3A_u minimum), in turn, explains why the dispersion component also favors the singlet state.

At first glance, it seems that the electrostatic component of the interaction energy (E_{el}) should also favor the singlet state. Indeed, the accumulation of positive charge in the superimposed PLYs of the triplet state (with respect to the charge distribution of the singlet state; see Figure 7 and Figure S4) should in principle lead to a strong electrostatic repulsion, thereby leading to a destabilization of this state. However, a Distributed Multipole Analysis[55] (DMA) brings to light not only that E_{el} is attractive in the ^3A_u minimum (E_{el} = −4.5 kcal/mol) but also that E_{el} is 1.4 kcal/mol more attractive in the triplet than in the singlet state (see Table S4).

An evaluation of the electrostatic interactions between the Mulliken charges of the different fragments of the SBP radicals in their π-dimers reveals that the surprising attractive electrostatic interaction in the triplet state is due to the fact that the sum of the two interactions between the superimposed PLY of one SBP radical and the spiro-linkage of the other radical that are present in a π-dimer is larger (in absolute terms) than the electrostatic repulsion between the two superimposed PLYs (see Table S5). On the other hand, the relative electrostatic stabilization of the triplet state (with respect to the singlet state) can be explained on the basis of the fact that

DOI: 10.1021/jacs.5b04053
J. Am. Chem. Soc. 2015, 137, 12843−12855

the attractive electrostatic interaction between the spiro linkages and the superimposed PLYs is larger when the fraction of positive charge localized in these PLYs increases (see Table S5). Let us stress that this also explains why the SBP unpaired electrons prefer to localize on the nonsuperimposed PLY rings in the triplet state. Indeed, this particular electron distribution entails an accumulation of positive charge on the superimposed PLY rings, which results in a larger electrostatic interaction energy by virtue of the zwitterionic nature of the SBP moieties. In fact, it is worth mentioning that the electrostatic component of the interaction energy at the optimum geometry of the triplet state is reduced down to −3.1 kcal/mol when it is evaluated using the distributed multipoles[55] of the singlet state. The observed decrease of 1.4 kcal/mol in the electrostatic interaction energy when switching from the electrostatic multipoles of the triplet to those of the singlet further corroborates that the localization of the unpaired electrons on the nonsuperimposed PLYs in the triplet state is driven by the electostatic interactions of the SBP radicals within the π-dimers.

In summary, our calculations reveal that the electrostatic component of the interaction energy between SBP radicals brings about a relative stabilization of the triplet state by about 1.4 kcal/mol. Remarkably, this relative stabilization is almost as large as the adiabatic gap between the triplet and singlet states (1.6 kcal/mol at the B3LYP-D2 level). It is thus concluded that the electrostatic interactions between SBP radicals play a prime role in stabilizing the triplet state and, thus, in enabling the spin transition observed in ethyl-SBP. These electrostatic interactions are also responsible for the localization of the SBP unpaired electrons on the nonsuperimposed PLYs of the π-dimers of ethyl-SBP above the spin-transition temperature. Therefore, the electrostatic interactions between SBP radicals constitute a crucial aspect for the understanding of the electronic structure and switching properties of ethyl-SBP.

CONCLUSIONS

The computational study herein presented provides new insights into the driving forces of the spin transition undergone by ethyl-SBP and into the key factors shaping the complex electronic structure of its building blocks, which are π-dimers of ethyl-substituted spiro-biphenalenyl (SBP) boron radicals. These SBP radicals are mixed-valence molecules whose unpaired electron in the electronic ground state is symmetrically delocalized over the two mutually perpendicular phenalenyl (PLY) units. Notwithstanding this delocalized ground state, our study reveals that the localization of the unpaired electron on one of the PLY units entails a very small energy penalty of ca. 1 kcal/mol, thereby providing a rationale for the large diversity of electronic structures observed in the SBP radicals of SBP-based organic conductors, including those SBPs that feature an asymmetric electron density distribution in spite of being monomeric in the solid state.[30]

Below the spin transition temperature, the structures of the π-dimers of ethyl-SBP are governed by the potential energy surface (PES) of the ground singlet state, whose minimum structure is characterized by a partial localization of the unpaired electrons of the SBPs in the superimposed PLY units. Above the spin transition temperature, the π-dimers adopt a configuration in which the unpaired electrons are localized on the nonsuperimposed PLY rings. Our calculations reveal that the topology of the PES in the region of this configuration is quite unique because this configuration only exists as a minimum in the PES of the ground triplet state. In the open shell singlet associated with this triplet state (i.e., a singlet state in which the nonsuperimposed PLYs host the unpaired electrons), the unpaired electrons flow from the nonsuperimposed PLYs to the superimposed PLYs in a barrierless process that results in a localization of the unpaired electrons in the latter type of PLYs. It thus follows that the structures of the π-dimers above the spin-transition temperature are exclusively governed by the potential energy surface of the ground triplet state, even if the corresponding open-shell singlet lies slightly below in energy.

Ethyl-SBP can undergo a spin transition at ∼140 K because of the very small adiabatic gap between the triplet state and the singlet state of its constituent π-dimers. The key factor behind this small gap, in turn, is the electrostatic interaction between SBP radicals in their π-dimers. Our study has brought to light that the electrostatic component of the interaction energy between SBP radicals is more attractive (by about 1.5 kcal/mol) in the triplet state than in the singlet state. This electrostatic stabilization of the triplet state partially counteracts the bonding and dispersion components of the interaction energy, which favor the singlet state, and is thus crucial in bringing the triplet state very close in energy to the singlet state, thereby enabling the spin transition observed in ethyl-SBP.

The electrostatic stabilization of the triplet state is counterintuitive because the larger fraction of positive charge hosted by the superimposed PLYs of the SBP π-dimer in this state (compared to the singlet) should in principle lead to a strong electrostatic repulsion. However, our analysis reveals that such electrostatic repulsion is counterbalanced by the attractive electrostatic interaction between these positively charged superimposed PLYs and the negatively charged boron-centered spiro linkages. Hence, the relative electrostatic stabilization of the triplet stated originates in the zwitterionic charge distribution of the SBP radicals. Such zwitterionic charge distribution also explains the localization of the unpaired electrons on the nonsuperimposed PLYs in the triplet state of the π-dimers. Indeed, the localization of spin density in the nonsuperimposed PLYs entails a localization of an excess of positive charge in the superimposed PLYs, thus giving rise to a larger attractive electrostatic interaction between SBP radicals in the π-dimers. On the other hand, the partial localization of the SBP unpaired electrons in the superimposed PLYs observed in the singlet state of the π-dimers stems from a delicate balance between the tendency of an isolated SBP radical to delocalize its spin density and the SOMO−SOMO overlap within the dimer, which favors the localization of the unpaired electrons in the superimposed PLYs (as the unpaired SBP electrons become more localized in the superimposed PLYs, the SOMO−SOMO overlap becomes larger and, consequently, the bonding component of the interaction energy between SBP radicals becomes stronger).

The unveiled prime role of the electrostatic interactions between SBP radicals in defining the electronic structure of the π-dimers of ethyl-SBP and driving its spin transition transcends the specific system herein studied. Indeed, the competition between the SOMO−SOMO overlap, which stabilizes the singlet states of the π-dimers, and the electrostatic interactions between radicals, which stabilizes the triplet states, constitutes a key concept to be reckoned with when it comes to rationalizing the electronic structure of the π-dimers present in the crystals of other members of the family of SBP-based conductors. Given the well-known exponential dependence of the SOMO−

DOI: 10.1021/jacs.5b04053
J. Am. Chem. Soc. 2015, 137, 12843−12855

SOMO overlap between radicals with their interplanar distance and their relative degree of slippage,[56−59] a small increase of these structural parameters due to crystal packing effects is expected to substantially reduce this overlap, thereby destabilizing the singlet state of the π-dimers and, consequently, leading to a smaller adiabatic gap between the triplet and singlet states. In the limiting case of a very large destabilization of the singlet, the electrostatic interactions can give rise to a nonswitchable material featuring π-dimers in the triplet state (with the unpaired electrons localized in the nonsuperimposed PLY units) in the whole range of temperatures, as observed for the following SBP-based materials: propyl-SBP,[15] pentyl-SBP,[16] octyl-SBP[18] and tetrathiomethyl- and tetrathioethyl-substituted SBPs.[27] On the other hand, a decrease of the interplanar distance should result in a larger SOMO−SOMO overlap, thereby stabilizing the singlet state of the π-dimers, thus leading to a larger adiabatic gap between the triplet and singlet states. This increase in the gap should in turn result in a shift of the transition temperature to higher values, as observed in the crystals of butyl-SBP.[12,51] Overall, the herein unveiled intricate interplay between spin delocalization, electrostatic interactions and SOMO−SOMO overlap allows for a better understanding of the intriguing electronic structure and switching properties of the π-dimers of spirobiphenalenyl-based radicals.

■ COMPUTATIONAL DETAILS

The calculations done using the CASSCF, RASSCF[60] (i.e., multiconfigurational SCF calculations using the Restricted Active Space construction of the wave function) and CASPT2[61] (i.e., second-order perturbation theory calculations based on a complete active space self-consistent field reference wave function) methods were carried out using the MOLCAS package.[62] Unless otherwise stated, atomic natural orbitals (ANO-S) basis sets[63] were employed in all these calculations, by using the following contraction levels: a [3s2p1d] contraction for the C, N, O, and B atoms, and a [2s] contraction for the H atoms. The Cholesky decomposition[64] (with a decomposition threshold of 1.0d-4) was used to treat the two-electron integrals in all the MOLCAS calculations. The CASPT2 calculations, in turn, were performed using the standard ionization potential electron affinity (IPEA) Hamiltonian.[65]

The NEVPT2[66] calculations (i.e., calculations based on *n*-electron valence state perturbation theory using a CASSCF reference wave function) were carried out using a 6-31G(d) basis set,[67] as implemented in the ORCA code.[68] The Resolution of the Identity approximation[69] was exploited to reduce the computational cost associated with these calculations.

Unless otherwise stated, all DFT calculations were done using the 6-31G(d) basis set,[67] as implemented in Gaussian09.[70] All DFT calculations were done using the spin-unrestricted approach.

It should be mentioned that in all the calculations dealing with isolated SBP radicals or isolated π-dimers, the ethyl groups of the SBP radicals were replaced with methyl groups to lower the cost of the calculations. In the following, we provide further details of the methodology employed to obtain the results presented in each subsection of the Results and Discussion.

(1). Electronic Structure of a Spirobiphenalenyl Neutral Radical. The molecular geometries employed to compute the energy profiles along the reaction coordinate (ξ) of the electron transfer between the two PLY units of an isolated SBP radical (Figure 3) were generated by means of a linear interpolation between the optimized structures associated with the electronic configurations having the unpaired electron of the SBP radical localized in either one or the other phenalenyl unit. These optimized structures were obtained using the M06-HF exchange-correlation functional.[71] Given the well-known tendency of Hartree−Fock calculations to localize charge and spin,[72] the optimized geometries of the asymmetric spin localized structures were computed using the M06-HF density functional,[71] which contains full Hartree−Fock exchange. This particular density functional contains also local correlation energy and is thus expected to furnish better optimized geometries than those that could be obtained with Hartree−Fock calculations.

The active space employed in the single point CASSCF(1,2) calculations along ξ includes one electron and the two phenalenyl SOMO orbitals. The CASSCF(1,2) wave functions employed to evaluate the spin density distribution along ξ (top graphic in Figure 3) and used as reference in the CASPT2 and NEVPT2 single point calculations along ξ (bottom graphic in Figure 3) were obtained by averaging the two lowest electronic states with equal weight. It is noted that the use of such state-average technique was previously reported to be crucial for the proper ab initio description of another organic mixed valence compound.[73,74] Likewise, previous studies demonstrated that both the nondynamical correlation (included in the CASSCF(1,2) calculations) and the dynamical correlation (which is captured at the CASPT2 or NEVPT2 levels) need to be taken into account for a reliable modeling of purely organic mixed-valence compounds.[72−74]

Concerning the performance of DFT, the bottom graphic of Figure 3 shows that the PBE and B3LYP functionals are able to provide a proper description of the electronic structure of an isolated SBP radical and, therefore, of the π-dimers of SBPs. For this reason, in this particular work, we have opted for not increasing the amount of Hartree−Fock exchange[75] or resorting to long-range corrected hybrid functionals while tuning their range-separation parameter,[76,77] as done in other works dealing with purely organic mixed valence compounds.

(2). Electronic Structure of the X-ray Crystal Structures of π-Dimers of SBP. The calculations aimed at elucidating the electronic structure of the SBP π-dimers were carried out at the CASSCF(2,4) level. The active space employed in these multireferent calculations includes two electrons (one for each unpaired electron of the two SBP radicals forming the dimer) distributed in four different orbitals (one for each SOMO of the four PLY units in the dimer).

The CASSCF(2,4) calculations done to obtain the wave function of the singlet ground state of A_g symmetry of the π-dimers of ethyl-SBP and to analyze its electronic structure were performed by averaging the three lowest singlet states of this particular symmetry with equal weight. The CASSCF(2,4) calculations to obtain the wave function of the lowest triplet state of A_u symmetry, in turn, were performed by averaging the three lowest triplet states of this particular symmetry with equal weight.

(3). Exploration of the Potential Energy Surface of the π-Dimers of SBPs: Mechanism of the Spin-Transition. The geometry optimizations of isolated SBP π-dimers were done while preserving the C_i symmetry of these dimers in the crystal. These optimizations were done at the B3LYP-D2 level (i.e., B3LYP calculations including Grimme's semiempirical dispersion potential in its D2 parametrization[78] to properly account for the van der Waals interactions between the two SBP radicals). The structures obtained upon optimization were characterized as minima by means of analytical vibrational frequency calculations. These vibrational frequencies were in turn used to obtain the temperature-dependence of the difference in entropy between the ^1A_g and ^3A_u states of an isolated SBP π-dimer within the harmonic approximation (Figure 9).

Plane wave pseudopotential calculations were employed for the structure optimizations of ethyl-SBP in the solid state. These calculations were carried out using the PBE exchange correlation functional[52] within the spin unrestricted formalism, together with Vanderbilt ultrasoft pseudopotentials[79] and Γ-point sampling of the Brillouin zone. The cell used in these calculations comprised two different π-dimers of ethyl-SBP. In these solid state calculations, the semiempirical dispersion potential introduced by Grimme (in its D2 parametrization[78]) was added to the conventional Kohn−Sham DFT energy in order to properly describe the van der Waals interactions between ethyl-SBP radicals. For the variable-cell optimizations (in which both the atomic positions and the lattice parameters were optimized), the plane wave basis set was expanded at a kinetic energy cutoff of 60 Ry. After the variable-cell relaxations, the corresponding optimized atomic positions and optimized lattice parameters for the LS and HT states of ethyl-SBP were used to define the initial

DOI: 10.1021/jacs.5b04053
J. Am. Chem. Soc. 2015, 137, 12843−12855

geometries for a subsequent optimization at a cutoff of 45 Ry in which the lattice parameters were kept fixed. These new optimizations with a smaller cutoff were performed to be able to carry out a finite-difference normal-mode analysis of the final optimized structures at a reasonable computational cost. These normal-mode analyses confirmed that the stationary points obtained were minima. In addition, the corresponding vibrational frequencies were used to evaluate the temperature-dependence of the difference in entropy between the HS and LS states of the π-dimers of ethyl-SBP in the solid state within the harmonic approximation (Figure 9). All the calculations in the condensed phase were carried out with the QUANTUM ESPRESSO package.[80] The calculations of ethyl-SBP in the solid state were performed with PBE because this functional is less demanding (in terms of computational cost) than B3LYP. Prior to these calculations, we confirmed that PBE-D2 calculations of the PESs for both the ^1A_g and ^3A_u states furnish the same topologies than those obtained at the B3LYP-D2 level (Figure S3).

(4). Key Role of Electrostatic Interactions in Driving the Spin Transition. The interaction energy decomposition analysis performed for the ^3A_u and the ^1A_g states of the π-dimers of ethyl-SBP was carried out using the intermolecular perturbation theory (IMPT) method for open shell molecules.[81,36] Assuming, as is commonly found, that the polarization (E_{pol}) and charge-transfer (E_{ct}) components of the IMPT interaction energy are 1 order of magnitude smaller that the remaining ones, the IMPT interaction energy between two open shell fragments, A and B, takes the expression:[36]

$$E_{int} \approx E_{er} + E_{el} + E_{disp} + E_{bond} \quad (1)$$

The terms of eq 1 have the following physical meaning: (1) E_{er} is the exchange-repulsion component that is always energetically repulsive in accord with the Pauli exclusion principle; (2) E_{el} is the electrostatic component of the nonpolarized system, which can be accurately approximated as a sum of classical multipoles (the charge−charge, charge−dipole, dipole−dipole, etc. components); (3) E_{disp} is the dispersion component, a nonclassical term that arises from the instantaneous dipole−dipole interactions resulting from the correlated motions of the electrons in A and B; and (4) E_{bond} is the bonding component, associated with the pairing of the unpaired electrons of fragments A and B. The form in which the different terms of eq 1 were evaluated for the π-dimers of ethyl-SBP is explained in detail in the footnotes of Table S4. Finally, it should be mentioned that the Distributed Multipole Analysis[55] aimed at evaluating the multipolar electrostatic component of the interaction energy was carried out with the GAMESS[82] suite of programs at the B3LYP/6-31g(d) level. The results obtained at the B3LYP level were confirmed by means of CASSCF(2,4) calculations (Table S4).

■ ASSOCIATED CONTENT

Supporting Information

The Supporting Information is available free of charge on the ACS Publications website at DOI: 10.1021/jacs.5b04053.

Benchmark calculations for the description of the electronic structure of an SBP radical; benchmark calculations to validate the methodolgy employed to describe the potential energy surface of the π-dimer of SBP; analysis of the electronic structure of the π-dimers of butyl-SBP; atomic coordinates of the optimized geometries reported in this work (PDF)

■ AUTHOR INFORMATION

Corresponding Author

*jordi.ribas.jr@gmail.com, j.ribas@ub.edu

Notes

The authors declare no competing financial interest.

■ ACKNOWLEDGMENTS

We acknowledge the Spanish Government for financial support (Projects MAT2011-25972 and MAT2014-54025-P) and a "Ramón y Cajal" fellowship to J.R.-A. We also acknowledge Universitat de Barcelona for a Ph.D grant to M.F., and BSC and CSUC for the allocation of massive computer time. Finally, we are thankful to the Catalan DURSI (Grant 2014SGR1422).

■ REFERENCES

(1) Miller, J. S. *Adv. Mater.* **2002**, *14*, 1105−1110.
(2) *Stable Radicals: Fundamentals and Applied Aspects of Odd-Electron Compounds*; Hicks, R., Ed.; Wiley: New York, 2010.
(3) Lahti, P. M. *Adv. Phys. Org. Chem.* **2011**, *45*, 93−169.
(4) Ratera, I.; Veciana, J. *Chem. Soc. Rev.* **2012**, *41*, 303−349.
(5) Haddon, R. C. *Nature* **1975**, *256*, 394−396.
(6) Morita, Y.; Suzuki, S.; Sato, K.; Takui, T. *Nat. Chem.* **2011**, *3*, 197−204.
(7) Nishida, S.; Morita, Y.; Fukui, K.; Sato, K.; Shiomi, D.; Takui, T.; Nakasuji, K. *Angew. Chem., Int. Ed.* **2005**, *44*, 7277−7280.
(8) Raman, K. V.; Kamerbeek, A. M.; Mukherjee, A.; Atodiresei, N.; Sen, T. K.; Lazic, P.; Caciuc, V.; Michel, R.; Stalke, D.; Mandal, S. K.; Blugel, S.; Munzenberg, M.; Moodera, J. S. *Nature* **2013**, *493*, 509−513.
(9) Ueda, A.; Suzuki, S.; Yoshida, K.; Fukui, K.; Sato, K.; Takui, T.; Nakasuji, K.; Morita, Y. *Angew. Chem., Int. Ed.* **2013**, *52*, 4795−4799.
(10) Pal, S. K.; Itkis, M. E.; Tham, F. S.; Reed, R. W.; Oakley, R. T.; Haddon, R. C. *Science* **2005**, *309*, 281−284.
(11) Morita, Y.; Suzuki, S.; Fukui, K.; Nakazawa, S.; Kitagawa, H.; Kishida, H.; Okamoto, H.; Naito, A.; Sekine, A.; Ohashi, Y.; Shiro, M.; Sasaki, K.; Shiomi, D.; Sato, K.; Takui, T.; Nakasuji, K. *Nat. Mater.* **2008**, *7*, 48−51.
(12) Itkis, M. E.; Chi, X.; Cordes, A. W.; Haddon, R. C. *Science* **2002**, *296*, 1443−1445.
(13) Chi, X.; Itkis, M. E.; Patrick, B. O.; Barclay, T. M.; Reed, R. W.; Oakley, R. T.; Cordes, A. W.; Haddon, R. C. *J. Am. Chem. Soc.* **1999**, *121*, 10395−10402.
(14) Chi, X.; Itkis, M. E.; Kirschbaum, K.; Pinkerton, A. A.; Oakley, R. T.; Cordes, A. W.; Haddon, R. C. *J. Am. Chem. Soc.* **2001**, *123*, 4041−4048.
(15) Chi, X.; Itkis, M. E.; Reed, R. W.; Oakley, R. T.; Cordes, A. W.; Haddon, R. C. *J. Phys. Chem. B* **2002**, *106*, 8278−8287.
(16) Chi, X.; Itkis, M. E.; Tham, F. S.; Oakley, R. T.; Cordes, A. W.; Haddon, R. C. *Int. J. Quantum Chem.* **2003**, *95*, 853−865.
(17) Chi, X.; Tham, F. S.; Cordes, A. W.; Itkis, M. E.; Haddon, R. C. *Synth. Met.* **2003**, *133*−*134*, 367−372.
(18) Liao, P.; Itkis, M. E.; Oakley, R. T.; Tham, F. S.; Haddon, R. C. *J. Am. Chem. Soc.* **2004**, *126*, 14297−14302.
(19) Pal, S. K.; Itkis, M. E.; Reed, R. W.; Oakley, R. T.; Cordes, A. W.; Tham, F. S.; Siegrist, T.; Haddon, R. C. *J. Am. Chem. Soc.* **2004**, *126*, 1478−1484.
(20) Mandal, S. K.; Itkis, M. E.; Chi, X.; Samanta, S.; Lidsky, D.; Reed, R. W.; Oakley, R. T.; Tham, F. S.; Haddon, R. C. *J. Am. Chem. Soc.* **2005**, *127*, 8185−8196.
(21) Mandal, S. K.; Samanta, S.; Itkis, M. E.; Jensen, D. W.; Reed, R. W.; Oakley, R. T.; Tham, F. S.; Donnadieu, B.; Haddon, R. C. *J. Am. Chem. Soc.* **2006**, *128*, 1982−1994.
(22) Pal, S. K.; Itkis, M. E.; Tham, F. S.; Reed, R. W.; Oakley, R. T.; Donnadieu, B.; Haddon, R. C. *J. Am. Chem. Soc.* **2007**, *129*, 7163−7174.
(23) Sarkar, A.; Pal, S. K.; Itkis, M. E.; Liao, P.; Tham, F. S.; Donnadieu, B.; Haddon, R. C. *Chem. Mater.* **2009**, *21*, 2226−2237.
(24) Bag, P.; Itkis, M. E.; Pal, S. K.; Donnadieu, B.; Tham, F. S.; Park, H.; Schlueter, J. A.; Siegrist, T.; Haddon, R. C. *J. Am. Chem. Soc.* **2010**, *132*, 2684−2694.
(25) Sarkar, A.; Pal, S. K.; Itkis, M. E.; Tham, F. S.; Haddon, R. C. *J. Mater. Chem.* **2012**, *22*, 8245−8256.
(26) Sarkar, A.; Itkis, M. E.; Tham, F. S.; Haddon, R. C. *Chem. - Eur. J.* **2011**, *17*, 11576−11584.

DOI: 10.1021/jacs.5b04053
J. Am. Chem. Soc. 2015, 137, 12843−12855

(27) Bag, P.; Pal, S. K.; Itkis, M. E.; Sarkar, A.; Tham, F. S.; Donnadieu, B.; Haddon, R. C. *J. Am. Chem. Soc.* **2013**, *135*, 12936−12939.
(28) Haddon, R. C.; Chichester, S. V.; Marshall, J. H. *Tetrahedron* **1986**, *42*, 6293−6300.
(29) Miller, J. S. *Angew. Chem., Int. Ed.* **2003**, *42*, 27−29.
(30) Haddon, R. C.; Sarkar, A.; Pal, S. K.; Chi, X.; Itkis, M. E.; Tham, F. S. *J. Am. Chem. Soc.* **2008**, *130*, 13683−13690.
(31) Pal, S. K.; Bag, P.; Sarkar, A.; Chi, X.; Itkis, M. E.; Tham, F. S.; Donnadieu, B.; Haddon, R. C. *J. Am. Chem. Soc.* **2010**, *132*, 17258−17264.
(32) Goto, K.; Kubo, T.; Yamamoto, K.; Nakasuji, K.; Sato, K.; Shiomi, D.; Takui, T.; Kubota, M.; Kobayashi, T.; Yakusi, K.; Ouyang, J. *J. Am. Chem. Soc.* **1999**, *121*, 1619−1620.
(33) Fukui, K.; Sato, K.; Shiomi, D.; Takui, T.; Itoh, K.; Gotoh, K.; Kubo, T.; Yamamoto, K.; Nakasuji, K.; Naito, A. *Synth. Met.* **1999**, *103*, 2257−2258.
(34) Takano, Y.; Taniguchi, T.; Isobe, H.; Kubo, T.; Morita, Y.; Yamamoto, K.; Nakasuji, K.; Takui, T.; Yamaguchi, K. *J. Am. Chem. Soc.* **2002**, *124*, 11122−11130.
(35) Small, D.; Zaitsev, V.; Jung, Y.; Rosokha, S. V.; Head-Gordon, M.; Kochi, J. K. *J. Am. Chem. Soc.* **2004**, *126*, 13850−13858.
(36) Mota, F.; Miller, J. S.; Novoa, J. J. *J. Am. Chem. Soc.* **2009**, *131*, 7699−7707.
(37) Suzuki, S.; Morita, Y.; Fukui, K.; Sato, K.; Shiomi, D.; Takui, T.; Nakasuji, K. *J. Am. Chem. Soc.* **2006**, *128*, 2530−2531.
(38) Mulliken, R. S.; Person, W. B. *Molecular Complexes*; Wiley & Sons: New York, 1969; Chapter 16.
(39) Huang, J.; Kertesz, M. *J. Phys. Chem. A* **2007**, *111*, 6304−6315.
(40) Huang, J.; Kertesz, M. *J. Am. Chem. Soc.* **2003**, *125*, 13334−13335.
(41) Taniguchi, T.; Kawakami, T.; Yamaguchi, K. *Polyhedron* **2005**, *24*, 2274−2279.
(42) Takenaka, M.; Taniguchi, T.; Kawakami, T.; Kitagawa, Y.; Okumura, M.; Yamaguchi, K. *Chem. Lett.* **2007**, *36*, 1000−1001.
(43) Small, D.; Rosokha, S. V.; Kochi, J. K.; Head-Gordon, M. *J. Phys. Chem. A* **2005**, *109*, 11261.
(44) Zaitsev, V.; Rosokha, S. V.; Head-Gordon, M.; Kochi, J. K. *J. Org. Chem.* **2006**, *71*, 520.
(45) Huang, J.; Kertesz, M. *J. Am. Chem. Soc.* **2006**, *128*, 1418−1419.
(46) Huang, J.; Kertesz, M. *J. Am. Chem. Soc.* **2007**, *129*, 1634−1643.
(47) Tian, Y.-H.; Kertesz, M. *J. Am. Chem. Soc.* **2010**, *132*, 10648−10649.
(48) Kolb, B.; Kertesz, M.; Thonhauser, T. *J. Phys. Chem. A* **2013**, *117*, 3642−3649.
(49) Hankache, J.; Wenger, O. S. *Chem. Rev.* **2011**, *111*, 5138−5178.
(50) Heckmann, A.; Lambert, C. *Angew. Chem., Int. Ed.* **2012**, *51*, 326−392.
(51) Robin, M.; Day, P. *Adv. Inorg. Chem. Radiochem.* **1968**, *10*, 247.
(52) (a) Perdew, J. P.; Burke, K.; Ernzerhof, M. *Phys. Rev. Lett.* **1996**, *77*, 3865. (b) Perdew, J. P.; Burke, K.; Ernzerhof, M. *Phys. Rev. Lett.* **1997**, *78*, 1396.
(53) (a) Becke, A. D. *Phys. Rev. A: At., Mol., Opt. Phys.* **1988**, *38*, 3098. (b) Becke, A. D. *J. Chem. Phys.* **1993**, *98*, 5648. (c) Lee, C.; Yang, W.; Parr, R. G. *Phys. Rev. B: Condens. Matter Mater. Phys.* **1988**, *37*, 785.
(54) Note that this value is given per π-dimer.
(55) Stone, A. J.; Alderton, M. *Mol. Phys.* **1985**, *56*, 1047−1064.
(56) Leitch, A. A.; Yu, X.; Winter, S. M.; Secco, R. A.; Dube, P. A.; Oakley, R. T. *J. Am. Chem. Soc.* **2009**, *131*, 7112−7125.
(57) Rota, J.-B.; Le Guennic, B.; Robert, V. *Inorg. Chem.* **2010**, *49*, 1230−1237.
(58) Vérot, M.; Bréfuel, N.; Pécaut, J.; Train, C.; Robert, V. *Chem. - Asian J.* **2012**, *7*, 380−386.
(59) Vela, S.; Deumal, M.; Shiga, M.; Novoa, J. J.; Ribas-Arino, J. *Chem. Sci.* **2015**, *6*, 2371−2381.
(60) Malmqvist, P.-Å.; Rendell, A.; Roos, B. O. *J. Phys. Chem.* **1990**, *94*, 5477.
(61) Andersson, K.; Malmqvist, P.-Å.; Roos, B. O. *J. Chem. Phys.* **1992**, *96*, 1218.
(62) Aquilante, F.; De Vico, L.; Ferré, N.; Ghigo, G.; Malmqvist, P.-Å.; Neogrády, P.; Pedersen, T. B.; Pitonak, M.; Reiher, M.; Roos, B. O.; Serrano-Andrés, L.; Urban, M.; Veryazov, V.; Lindh, R. *J. Comput. Chem.* **2010**, *31*, 224.
(63) Pierloot, K.; Dumez, B.; Widmark, P.-O.; Roos, B. O. *Theor. Chim. Acta* **1995**, *90*, 87.
(64) (a) Beebe, N. H. F.; Linderberg, J. *Int. J. Quantum Chem.* **1977**, *12*, 683. (b) Røeggen, I. R.; Wisløff-Nielsen, E. *Chem. Phys. Lett.* **1986**, *132*, 154. (c) Koch, H.; Sańchez de Meraś, A.; Pedersen, T. B. *J. Chem. Phys.* **2003**, *118*, 9481. (d) Aquilante, F.; Pedersen, T. B.; Lindh, R. *J. Chem. Phys.* **2007**, *126*, 194106. (e) Aquilante, F.; Malmqvist, P.Å.; Pedersen, T. B.; Ghosh, A.; Roos, B. O. *J. Chem. Theory Comput.* **2008**, *4*, 694−702.
(65) Ghigo, G.; Roos, B. O.; Malmqvist, P.-Å. *Chem. Phys. Lett.* **2004**, *396*, 142.
(66) (a) Angeli, C.; Cimiraglia, R.; Malrieu, J.-P. *Chem. Phys. Lett.* **2001**, *350*, 297. (b) Angeli, C.; Cimiraglia, R.; Evangelisti, S.; Leininger, T.; Malrieu, J.-P. *J. Chem. Phys.* **2001**, *114*, 10252. (c) Angeli, C.; Cimiraglia, R.; Malrieu, J.-P. *J. Chem. Phys.* **2002**, *117*, 9138.
(67) Dietchfield, R.; Hehre, W. J.; Pople, J. A. *J. Chem. Phys.* **1971**, *54*, 724.
(68) Neese, F *ORCA— An ab Initio, Density Functional and Semiempirical Program Package*, Version 2.9; Max Planck Institute for Bioinorganic Chemistry: Müllheim, 2012.
(69) Neese, F. *J. Comput. Chem.* **2003**, *24*, 1740.
(70) Frisch, M. J.; Trucks, G. W.; Schlegel, H. B.; Scuseria, G. E.; Robb, M. A.; Cheeseman, J. R.; Scalmani, G.; Barone, V.; Mennucci, B.; Petersson, G. A.; Nakatsuji, H.; Caricato, M.; Li, X.; Hratchian, H. P.; Izmaylov, A. F.; Bloino, J.; Zheng, G.; Sonnenberg, J. L.; Hada, M.; Ehara, M.; Toyota, K.; Fukuda, R.; Hasegawa, J.; Ishida, M.; Nakajima, T.; Honda, Y.; Kitao, O.; Nakai, H.; Vreven, T.; Montgomery, J. A., Jr.; Peralta, J. E.; Ogliaro, F.; Bearpark, M.; Heyd, J. J.; Brothers, E.; Kudin, K. N.; Staroverov, V. N.; Kobayashi, R.; Normand, J.; Raghavachari, K.; Rendell, A.; Burant, J. C.; Iyengar, S. S.; Tomasi, J.; Cossi, M.; Rega, N.; Millam, N. J.; Klene, M.; Knox, J. E.; Cross, J. B.; Bakken, V.; Adamo, C.; Jaramillo, J.; Gomperts, R.; Stratmann, R. E.; Yazyev, O.; Austin, A. J.; Cammi, R.; Pomelli, C.; Ochterski, J. W.; Martin, R. L.; Morokuma, K.; Zakrzewski, V. G.; Voth, G. A.; Salvador, P.; Dannenberg, J. J.; Dapprich, S.; Daniels, A. D.; Farkas, Ö.; Foresman, J. B.; Ortiz, J. V.; Cioslowski, J.; Fox, D. J. *Gaussian 09*, Revision D.01; Gaussian, Inc.: Wallingford, CT, 2009.
(71) Zhao, Y.; Truhlar, D. G. *J. Phys. Chem. A* **2006**, *110*, 13126−13130.
(72) Kaupp, M.; Renz, M.; Parthey, M.; Stolte, M.; Würthner, F.; Lambert, C. *Phys. Chem. Chem. Phys.* **2011**, *13*, 16973−16986.
(73) Helal, W.; Evangelisti, S.; Leininger, T.; Maynau, D. *J. Comput. Chem.* **2009**, *30*, 83−92.
(74) Pastore, M.; Helal, W.; Evangelisti, S.; Leininger, T.; Malrieu, J.-P.; Maynau, D.; Angeli, C.; Cimaraglia, R. *J. Chem. Phys.* **2008**, *128*, 174102.
(75) Renz, M.; Theilacker, K.; Lambert, C.; Kaupp, M. *J. Am. Chem. Soc.* **2009**, *131*, 16292−16302.
(76) Sutton, C.; Körzdörfer, T.; Coropceanu, V.; Brédas, J.-L. *J. Phys. Chem. C* **2014**, *118*, 3925−3934.
(77) Körzdörfer, T.; Brédas, J.-L. *Acc. Chem. Res.* **2014**, *47*, 3284−3291.
(78) Grimme, S. *J. Comput. Chem.* **2006**, *27*, 1787−1799.
(79) Vanderbilt, D. *Phys. Rev. B: Condens. Matter Mater. Phys.* **1990**, *41*, 7892−7895.
(80) Giannozzi, P.; Baroni, S.; Bonini, N.; Calandra, M.; Car, R.; Cavazzoni, C.; Ceresoli, D.; Chiarotti, G. L.; Cococcioni, M.; Dabo, I.; Dal Corso, A.; Fabris, S.; Fratesi, G.; de Gironcoli, S.; Gebauer, R.; Gerstmann, U.; Gougoussis, C.; Kokalj, A.; Lazzeri, M.; Martin-Samos, L.; Marzari, N.; Mauri, F.; Mazzarello, R.; Paolini, S.; Pasquarello, A.; Paulatto, L.; Sbraccia, C.; Scandolo, S.; Sclauzero, G.; Seitsonen, A. P.;

DOI: 10.1021/jacs.5b04053
J. Am. Chem. Soc. 2015, 137, 12843−12855

Smogunov, A.; Umari, P.; Wentzcovitch, R. M. *J. Phys.: Condens. Matter* **2009**, *21*, 395502 (Quantum ESPRESSO v. 4.2.1)..
(81) Hayes, I. C.; Stone, A. J. *Mol. Phys.* **1984**, *53*, 83−105.
(82) Schmidt, M. W.; Baldridge, K. K.; Boatz, J. A.; Elbert, S. T.; Gordon, M. S.; Jensen, J. H.; Koseki, S.; Matsunaga, N.; Nguyen, K. A.; Su, S. J.; Windus, T. L.; Dupuis, M.; Montgomery, J. A. *J. Comput. Chem.* **1993**, *14*, 1347.

DOI: 10.1021/jacs.5b04053
J. Am. Chem. Soc. 2015, 137, 12843−12855